frontiers in Materials

ORIGINAL RESEARCH
published: 07 February 2020
doi: 10.3389/fmats.2020.00022

First-Principles Insight Into Au-Doped MoS_2 for Sensing C_2H_6 and C_2H_4

Guochao Qian[1,2], *Qingjun Peng*[1], *Dexu Zou*[1], *Shan Wang*[1], *Bing Yan*[1] *and Qu Zhou*[3]*

[1] Electric Power Science Research Institute of Yunnan Power Grid Co., Ltd., Kunming, China, [2] State Key Laboratory of Power Transmission Equipment and System Security and New Technology, Chongqing University, Chongqing, China, [3] College of Engineering and Technology, Southwest University, Chongqing, China

C_2H_6 and C_2H_4 gases are two typical decompositions produced by partial discharge of transformer oil. To fully evaluate the feasibility of MoS_2-based materials for the detection of C_2H_6 and C_2H_4 gases, the adsorption of C_2H_6 and C_2H_4 molecules on intrinsic and Au-doped MoS_2 monolayer have been studied in this paper by the First-principle of Density Functional Theory (DFT). The adsorption mechanism of MoS_2-based monolayer were investigated carefully in terms of adsorption energy, adsorption distance, bandgap structure, charge transfer and density of states (DOS). The calculated results show that the adsorption structures of the C_2H_6 and C_2H_4 molecules on Au-doped MoS_2 monolayer with larger adsorption energies were stable, and have shorter adsorption distance, higher charge transfer, and stronger orbital hybridization compared with the corresponding MoS_2 monolayer adsorption structures. It is concluded that the doped-Au atom affects the electronic structure of MoS_2 monolayer to enhance the adsorption capacity. From this aspect, the present research offers a theoretical guidance to the application of Au-doped MoS_2 materials as the sensing material for C_2H_6 and C_2H_4 gases.

Keywords: adsorption, Au-doped MoS_2 monolayer, DFT calculation, dissolved gases, gas sensors

OPEN ACCESS

Edited by:
Anita Lloyd Spetz, Linköping University, Sweden

Reviewed by:
Lars Ojamäe, Linköping University, Sweden
Karin Larsson, Uppsala University, Sweden

***Correspondence:**
Qu Zhou
zhouqu@swu.edu.cn

Specialty section:
This article was submitted to Translational Materials Science, a section of the journal Frontiers in Materials

Received: *18 October 2019*
Accepted: *20 January 2020*
Published: *07 February 2020*

Citation:
Qian G, Peng Q, Zou D, Wang S, Yan B and Zhou Q (2020) First-Principles Insight Into Au-Doped MoS_2 for Sensing C_2H_6 and C_2H_4. Front. Mater. 7:22. doi: 10.3389/fmats.2020.00022

INTRODUCTION

The transformers are considered to be the most important equipment in the power system, which affects the running state of power transmission (Chen W. G. et al., 2013; Ma H. et al., 2015; Uddin et al., 2016). After a long period of operation, the security and reliable operation ability of power transformers will be weakened due to inevitable defects, which will bring about power accidents and cause great inconvenience to the citizens and the society (Ma G. M. et al., 2015; Nobrega et al., 2019). Currently, failures within an oil-immersed transformer will cause the oil to decompose into several characteristic gases dissolved in it, including H_2, CO, CO_2, C_2H_2, CH_4, C_2H_6, and C_2H_4. Some minor faults in the transformers may lead to the spark discharge in the transformer oil, then cause the oil decompose and produces C_2H_6, C_2H_4 gases (Benounis et al., 2008; Yang et al., 2011). Therefore, dissolved gas analysis (DGA) to monitor dissolved gas in transformer oil is regarded to be the most direct method to guarantee the stable running of power transformer or to predict some fault trends (Chatterjee et al., 2013; Suryavanshi et al., 2017; Cun et al., 2019; de Lima et al., 2019).

In recent decades, metal inorganic compound semiconductor sensors have been widely used in the field of gas detection (Zhang et al., 2017c; Zhou et al., 2018c, 2019; Chao et al., 2019; Kim et al., 2019, 2020; Wang et al., 2019c, 2020). Among them, nanowires or fiber materials sensors have attracted extensive attention due to their high sensitivity, fast response and recovery, low power consumption, and other excellent properties. The high sensitivity of nanowires or fiber materials sensors can be attributed to the large number of adsorption sites provided by high specific surface area (Chen X. et al., 2013; Qin and Ye, 2016; Wang et al., 2018). Molybdenum disulfide (MoS_2) belongs to hexagonal crystal system and is a typical transition metal sulfide with a lamellar structure similar to graphene, which has the characteristics of surface effect, small size effect and quantum effect, and large specific surface area (Zhang et al., 2017b; Chen et al., 2019a). In addition, some studies have proved that nanometer MoS_2, with excellent performances in adsorption capacity and other aspects, which is a special source of gas storage materials or sensing materials (Wen et al., 2016; Zhang et al., 2017a; Zhang D. Z. et al., 2018; Zhang Y. J. et al., 2018; Zhou et al., 2018b).

At present, the sensitivity or selectivity of most sensors are limited to some extent. In order to promote the sensing performance of gas sensors, dopant is usually used to enhance electron mobility and chemical reactivity of sensing materials. For instance, Zhou at al. verified that Pt nanoparticles doped SnO_2 nanoneedles can be an effective gas sensing material for the detection of CO, which exhibits excellent response and recovery characteristic and remarkable selectivity (Zhou et al., 2018d). Zhang et al. studied the behavior of a MoS_2/Co_3O_4-based ammonia gas sensor. They concluded that the MoS_2/Co_3O_4 gas sensor exhibited excellent sensitivity performance to low-concentration ammonia, which is better than the pure Co_3O_4 gas sensor (Zhang et al., 2017a). Zhou at al. synthesized pure and Ni doped SnO_2 nanomaterials and found the Ni doped SnO_2 gas sensor shows lower optimum operating temperature and superior sensitivity properties to CO compared with the pure one (Zhou et al., 2018a).

Density functional theory (DFT) is a method to calculate the atomic or electronic structure and characteristic information of a material system by first-principles (Zhao and Wu, 2018; Wang et al., 2019c). Moreover, it has been widely employed to effectively predict the sensing properties of materials or interpret sensing mechanisms. Wang et al. analyzed the influence of Ni atom on the adsorption properties of ZnO (100) surface by using DFT calculations and found the doped Ni atom, as the active site, significantly enhance the adsorbability of SO_2, SOF_2, SO_2F_2 gases (Wang et al., 2019a). Zahra et al. investigated the adsorption of H_2S on transition element (such as Ni, Cu, and Zn) atom-doped graphene based on DFT and concluded that the adsorption configuration of the H_2S molecule near the dopant on the doped graphene surface is most stable (Zahra, 2018). Esrafili et al. used DFT to analyze the sensing mechanism of C-doped h-BN nanosheets, and the results indicated that the sensing of NO and NO_2 can be selectively conducted in the presence of CO, H_2O, CO_2, and NH_3 gases (Esrafili and Rad, 2019). Many studies have reported the performance and mechanism of MoS_2-based gas sensors. However, MoS_2 based fiber-materials as the gas sensor to detect transformer oil dissolved-gases has hardly been studied theoretically and experimentally.

In this study, Au was employed as a dopant to change the structural characteristics and electronic properties of MoS_2 fiber-materials, and the adsorption performance of Au-doped MoS_2 to C_2H_6 and C_2H_4 gases was investigated through DFT study. The stable adsorption structures of C_2H_6 and C_2H_4 molecules on intrinsic or Au-doped MoS_2 monolayer were built. Furthermore, the adsorption energies, charge transfer, adsorption distance, density of states, and bandgap have been calculated to comprehensively investigate the adsorption abilities of Au-doped MoS_2 monolayer to C_2H_6 and C_2H_4 gases. The results of this research have important guiding significance for the design of high efficiency MoS_2 fiber based sensors to detect fault characteristic gas in transformer oil (C_2H_6 and C_2H_4 gases).

CALCULATION DETAILS

All the First-principles calculations in this study were processed in $Dmol^3$ package of Materials Studio software based on DFT. General Gradient Approximate (GGA) of Perdew-Burke-Ernzerhof (PBE) were selected to optimize the geometric and calculate the exchange-correlation energy (Qian et al., 2019). The double numerical plus polarization (DNP) and the density functional semi-core pseudopotential (DSPP) were taken to processed the core electron. In addition, the k-point grid was generated according to the Monkhorst-Pack scheme and the sampling k point of Brillouin zone was set to $5 \times 5 \times 1$. The self-consistent field (SCF) convergence precision was set to 1×10^{-6} Ha and the DIIS was set to 6 to shorten the convergence time of SCF. The convergence tolerance, maximum force and maximum displacement were set to 1×10^{-5} Ha, 2×10^{-3} Ha/Å, and 5×10^{-3} Ha in the geometry optimization processes. All simulations results in present study were based on a $4 \times 4 \times 1$ MoS_2 supercell with 48 atoms (including 32 S atoms and 16 Mo

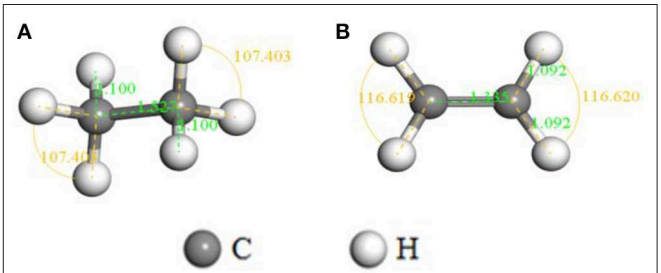

FIGURE 1 | The structures of **(A)** C_2H_4 and **(B)** C_2H_2.

TABLE 1 | The Mulliken atomic charges of gas molecules.

Gas molecule	C	H
C_2H_6	−0.142	0.047
C_2H_4	−0.101	0.050

atoms). With regard to the periodic boundary conditions (PBC), a vacuum layer in z-direction of 20 Å, which is perpendicular to the xy-plane, was employed to prevent the interaction between the adjacent layers.

The adsorption energy (E_{ads}) of gases (C_2H_6, C_2H_4, and C_2H_2) on the pristine or Au-doped MoS_2 monolayer is defined in Equation (1) (Chen et al., 2019b).

$$E_{ads} = E_{total} - E_{monolayer} - E_{gas} \quad (1)$$

where E_{total}, $E_{monolayer}$, and E_{gas} are the energy of pristine or Au-doped MoS_2 monolayer adsorbed system, corresponding monolayer and gas molecule, respectively. A negative adsorption energy represents spontaneous adsorption. The amount of charge transfer (Q_t) can be obtained based on the Mulliken analysis, and Q_t is calculated by Equation (2) (Chen et al., 2015).

$$Q_t = Q_a - Q_b \quad (2)$$

where Q_a and Q_b are the carried charge of the adsorbed gas and the isolated gas. A positive Q_t suggests the gas accept charges from monolayer during the adsorption.

RESULTS

Properties of Gas Molecules and MoS_2 Monolayer

The optimized structures with corresponding parameters of C_2H_6 and C_2H_4 are shown in **Figure 1**. The bond length of C-C, C-H in C_2H_6 are 1.527 and 1.100 Å, and the bond angle of H-C-H is 107.4°. For C_2H_4 molecule, the structure is symmetric around the C-C bond (the length is 1.335 Å), the H-C-H angle is 116.6° and the length of C-H bond is similar to C_2H_6, which is 1.092 Å. Mulliken atomic charge analysis (**Table 1**) exhibits that the C atom of C_2H_6 molecule has negative charges of −0.868e, while the carried charges of H atoms is 0.047e. The carried charges of C and H atoms in C_2H_4 are −0.101e and 0.050e. It can be concluded that the electrons of C atoms are transferred from H atoms, which indicates the interaction between C atoms and H atoms.

The optimized structure of MoS_2 monolayer model with the lattice parameters of 12.424, 12.584, and 18.152 Å in the a, b, and c directions, as shown in **Figure 2A**. Besides, the optimized bond angles of S-Mo-S and Mo-S-Mo are achieved as 81.5°, which are comparable to 81.5° in previous study (Wang et al., 2019b). The electronic structural characteristics of MoS_2 monolayer were investigated, the relevant band gap structure and DOSs are

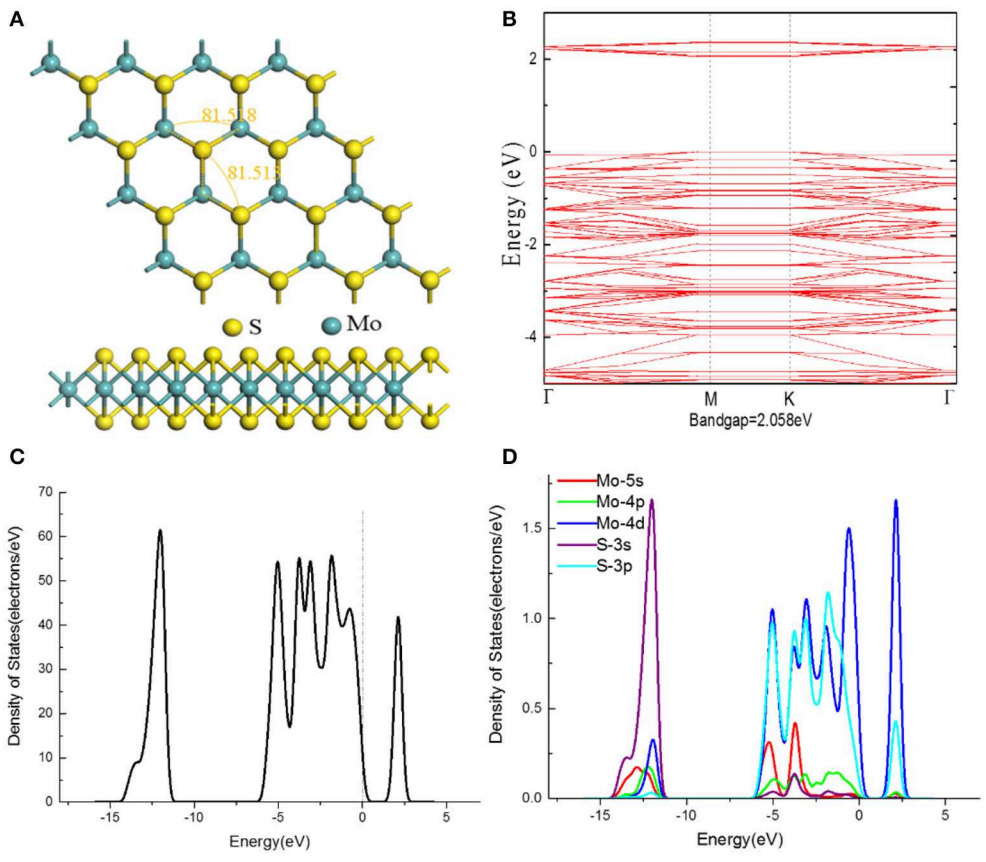

FIGURE 2 | (A) The structures, **(B)** Band structures, **(C)** TDOS, and **(D)** PDOS of MoS_2 monolayer.

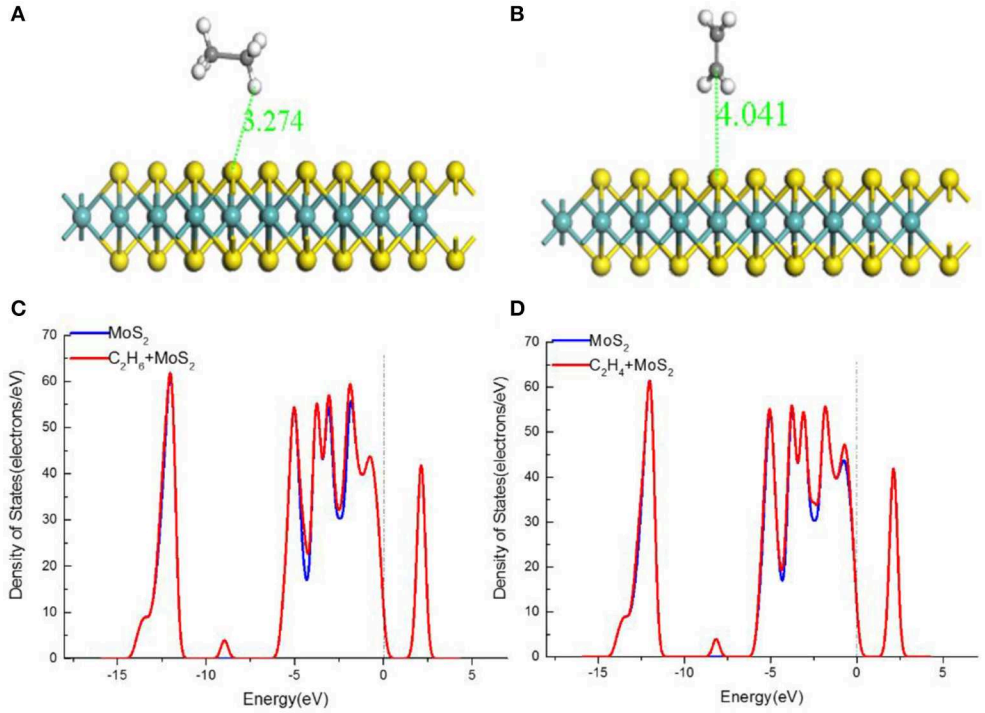

FIGURE 3 | The structures of MoS_2 monolayer of **(A)** C_2H_6-adsorbed MoS_2 monolayer, **(B)** C_2H_4-adsorbed MoS_2 monolayer and the TDOS of **(C)** C_2H_6-adsorbed MoS_2 monolayer, **(D)** C_2H_4-adsorbed MoS_2 monolayer.

shown in **Figures 2B–D**. It is easily to distinguish the valence band maximum (VBM) and conduction band minimum (CBM), and the Fermi level (represented by the line of zero energy) is located in the energy bandgap. As a result, the considered MoS_2 monolayer with band gap of 2.058 eV is observed to be a direct band semiconductor. The total density of state in **Figure 2C** is composed of the conduction band, upper valence band, and lower valence band with energy values of 1.9∼2.5 eV, −5.8∼0 eV, and −14∼−11.8 eV, respectively. According to the PDOS in **Figure 2D**, the conduction band is mainly dominated by 4d-orbital of Mo atom, while the 4p, 4d-orbitals of Mo atom and 3s, 3p-orbitals of S atom contribute to the valence band.

Adsorption Properties of Molecules on MoS_2 Monolayer

The C_2H_6, C_2H_4, and C_2H_2 molecules were placed above the MoS_2 monolayer, the optimized adsorption structures and DOSs are shown in **Figure 3**. **Table 2** reports the corresponding adsorption energy (E_{ads}), charge transfer (Q_t), adsorption distance (d), and band gap (E_g). As exhibited in **Figures 3C,D**, the density of state of two adsorption systems change only slightly. In addition, the E_{ads} of C_2H_6, C_2H_4, and C_2H_2 adsorbed MoS_2 monolayer are only −0.082, −0.106, and −0.101 eV, the corresponding Q_t and the change of band gap are very small, which clearly suggests that the adsorptions belong to physical adsorption with Van der Waals force. In conclusion, the C_2H_6, C_2H_4, and C_2H_2 gases are difficult to be stably adsorbed on pristine MoS_2 monolayer at room temperature, because the material is theoretically not active enough to adsorb them.

TABLE 2 | The parameters of MoS_2 monolayer adsorption structures.

Gas molecule	E_{ads} (eV)	Q_t (e)	d (Å)	E_g (eV)
C_2H_6	−0.082	0.018	3.274	2.057
C_2H_4	−0.106	0.002	4.041	2.056

Properties of Au-Doped MoS_2 Monolayer

According to the previous research, it is the stable doped position that putting Au atom on the top of the Mo atom. As shown in **Figure 4A**, three Au-S bonds with the same length of 2.809 Å have been formed and the distance (3.749 Å) between Au and Mo atoms is too far to form bond due to the weak interaction. Compared with the undoped structure, the bond angle of Mo–S–Mo (80.8°) and S–Mo–S (81.3°) in Au doped MoS_2 monolayer have slightly decreases. The carried electrons of the Au atom to MoS_2 monolayer was calculated to 0.043e, suggesting the interaction between Au atom and the surface of MoS_2 monolayer leads to a steady doping structure.

For the PDOS (**Figure 4D**) of doped system, it can be found there is large overlap area from −3.7 to 0 eV of S-3p orbital and Au-5d orbital, verifying that strong hybridization occurs between S-3p and Au-5d orbitals. It can be inferred

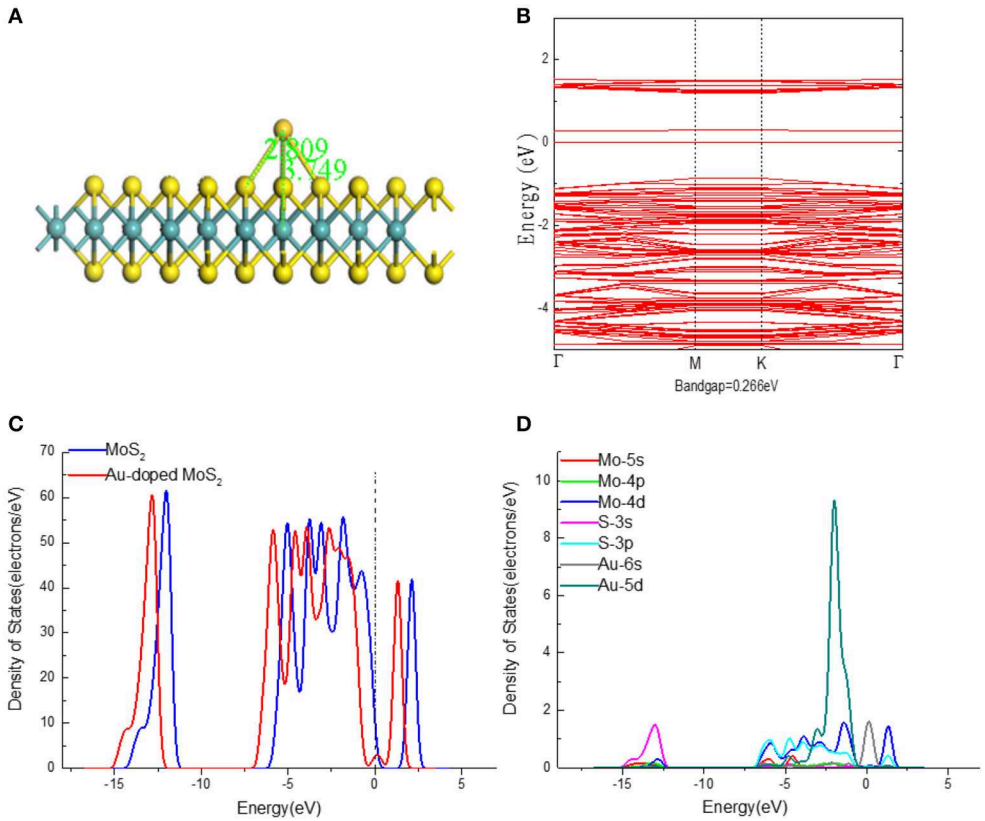

FIGURE 4 | (A) The structures, **(B)** Band structures, **(C)** TDOS, and **(D)** PDOS of Au-doped MoS_2 monolayer.

that chemical interaction exists between the doped Au atom and MoS_2 to promote the formation of the final stable doping structure. **Figure 4C** shows the waveform of DOS has barely changed except for the obvious left shift after the dope of Au atom, which not only indicates an increase in the amount of system electrons, but means a promotion in the metallicity. The Au-doping introduces some impurity energy levels from the Au-6s and 5d orbitals into the band gap, leading to a narrowing of the bandgap (0.266 eV), which is corresponding with **Figure 4B**. The smaller band gap implies the lower kinetic stability and the higher chemical activity. Therefore, Au-doping makes the transfer from valence band to conduction band of electrons become easier, thus the conductivity and reactivity are improved.

Adsorption Properties of Molecules on Au-Doped MoS_2 Monolayer

To investigate the adsorption properties of Au-doped MoS_2 monolayer to C_2H_6 molecule, a C_2H_6 was placed at different positions to close the Au atom, and geometric optimization was conducted. The most stable structure is shown in **Figure 5A**, the corresponding adsorption energy, charge transfer, adsorption distance and band gap of this adsorption configurations are listed in **Table 3** and the density of states (DOS) are illustrated in **Figures 5B–D**.

The C_2H_6 molecule was trapped at the Au doping site and the distance between Au atom and C atom is 2.757 Å, which is significantly smaller than that in MoS_2 monolayer adsorption system (3.274 Å). Besides, it can be found that the structure of C_2H_6 molecule changes little after being adsorbed by Au-doped MoS_2 monolayer, while the change of the Au-S bonds is clearly observed. According to **Table 3**, the adsorption energy is −0.463 eV, which is greater than the intrinsic adsorption structure. Moreover, the value of transferred electrons that calculated by Mulliken analysis is 0.118e, indicating the Au–MoS_2 monolayer acts as an acceptor for the electrons transferred from the C_2H_6 molecule. It is observed that the band gap of Au-doped MoS_2 monolayer system reduce from 0.266 to 0.206 eV. Therefore, the conclusion that the C_2H_6 molecule was adsorbed on the Au–MoS_2 monolayer by chemisorption is obtained.

To further explore the adsorption mechanism between the Au–doped MoS_2 monolayer and C_2H_6 molecule, the total density of states (TDOS) and the projected density of states (PDOS) of the adsorption system are analyzed in detail. Adsorption is mainly affected by the outer atomic orbitals, hence the Mo-5s, Mo-4d, S-3s, S-3p, Au-5d, C-2s, and H-1s orbitals were investigated, as shown in **Figure 5D**. Distinctly, some changes of TDOS after C_2H_6 adsorption can be observed in **Figure 5B**, such as the increases around the Fermi level, which may be consistent

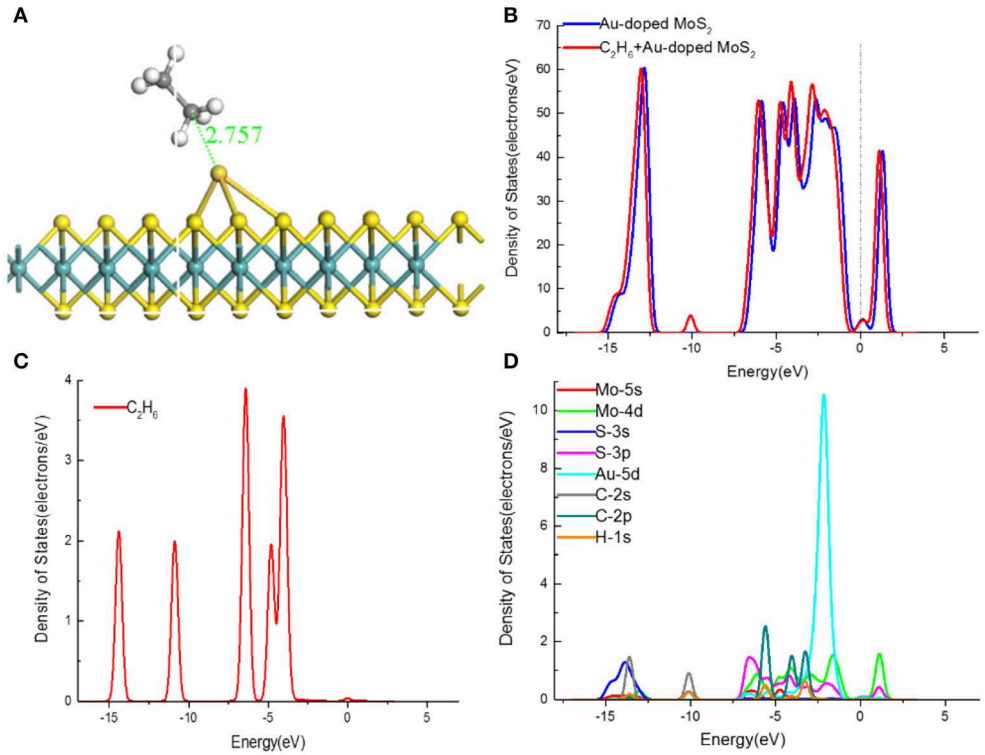

FIGURE 5 | (A) The structures, **(B)** TDOS, **(D)** PDOS of C_2H_6-adsorbed MoS_2 monolayer, and **(C)** the TDOS of C_2H_6 molecular.

with the reduction of the bandgap. It can be deduced that this phenomenon is due to the introduction of impurity energy level caused by a large amount of electrons transfer in the adsorption. In addition, a narrower bandgap suggests the adsorption structure conducts electricity better and the electrons are more easily to transfer. The TDOS has a left shift and some new peaks at −10 and −2.4 eV appear. By the comparison with **Figure 5C**, it can be found that the changes of TDOS are influenced by the C_2H_6 molecule and the slight peak near the Fermi level in the DOS of C_2H_6 contributes to the decrease of the bandgap, particularly. Moreover, it can be implied that some orbitals hybridization occur to the C_2H_6 adsorption Au–doped MoS_2 monolayer system. **Figure 5D** concludes that the C-2p, Mo-4d and Au-5d orbitals dominate the changes of TDOS. The H-1s and Au-5d overlap around −3 eV, while the obvious overlapping region of C-2p, Mo-4d, and Au-5d orbitals at −5.5 and −2.5 eV. The PDOS overlap of the orbitals indicates hybridization happen between them. Therefore, it can be concluded by the contribution of the C-2p orbitals that during the adsorption process, the Au–doped MoS_2 monolayer mainly adsorbs C_2H_6 molecule by capturing C atom.

Above all, the Au–doped MoS_2 monolayer has a large adsorption energy, more transferred electrons, short adsorption distance and more obvious orbitals hybridization than the corresponding intrinsic adsorption system. In conclusion, the adsorption performance of MoS_2 monolayer has a significant improvement after Au doped and the doped structure can effectively absord the C_2H_6 molecule.

TABLE 3 | The parameters of Au-doped MoS_2 monolayer adsorption structures.

Gas molecule	E_{ads} (eV)	Q_t (e)	d (Å)	E_g (eV)
C_2H_6	−0.463	0.118	2.757	0.206
C_2H_4	−0.952	0.309	2.170	0.122

For C_2H_4 molecule adsorption on Au-doped MoS_2 monolayer, the most stable adsorption structure is presented in **Figure 6A**, where the molecule was adsorbed by the direction of parallel to MoS_2 monolayer. The adsorption properties parameters are classified at **Table 3**.

The adsorption of C_2H_4 molecule is characterized by a large negative adsorption energy (−0.952 eV), suggesting the chemical adsorption happen to the C_2H_4 molecule and Au-doped MoS_2 monolayer. By comparing with the adsorption on pristine MoS_2 monolayer, the higher adsorption energy implies that the interaction is stronger. Moreover, it can be noticed that the adsorption distance between doped Au atom and C atom in C_2H_4 molecule is 2.170 Å, illustrating the formation of Au-C covalent bond. Additionally, the amount of transferred charges in this adsorption system is 0.309e. The reorganization of charges indicates that the Au-doped MoS_2 monolayer acquires charges from C_2H_4 molecule. It is observed the charge transfer is much larger than the corresponding pristine MoS_2 monolayer adsorption structure, which indicates the dope of Au atom make

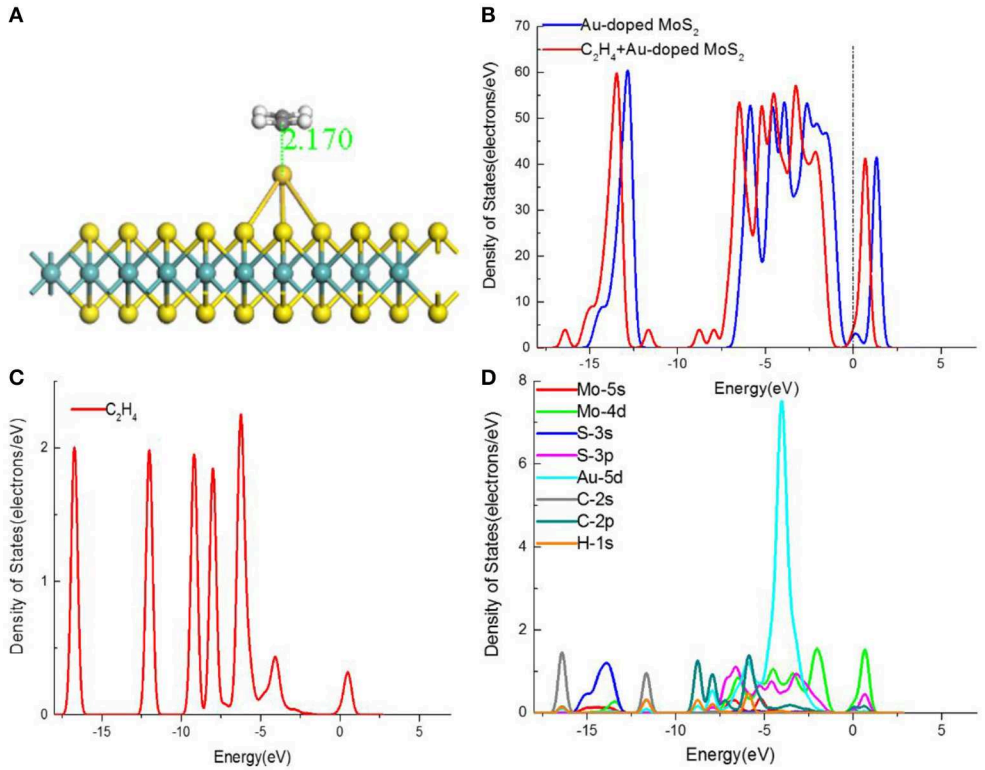

FIGURE 6 | (A) The structures, **(B)** TDOS, **(D)** PDOS of C_2H_4-adsorbed MoS_2 monolayer, and **(C)** the TDOS of C_2H_4 molecular.

the adsorption reaction between monolayer and C_2H_4 stronger. The band gap is decreased to 0.122 eV compared with that of Au-doped MoS_2 monolayer (0.266 eV), and the change represents the C_2H_4 molecule has the influence on the electronic structure of monolayer. In a conclusion, the C_2H_4 molecule could be detected effectively by the Au-doped MoS_2 monolayer.

The DOS and PDOS of C_2H_4 molecule adsorbed Au–doped MoS_2 monolayer were conducted to understand the effect of the C_2H_4 on the electronic properties of Au–doped MoS_2 monolayer. Adsorption is mainly affected by the outer atomic orbitals, hence the Mo-5s, Mo-4d, S-3s, S-3p, Au-5d, C-2s, and H-1s orbitals were investigated, as shown in **Figure 6D**. From **Figure 6A**, it is observed that the DOS of adsorption system has a certain displacement compared with the Au–doped MoS_2 monolayer, in which there is the apparent transition near the Fermi level. Furthermore, the bandgap decreased after the adsorption of C_2H_4 molecule, indicating the transfer of electrons between the conduction band and the valance band is easier. The DOS shifts to a lower region, which is consistent well with the charges accepting behavior of Au–doped MoS_2 monolayer. To be specific, the electron density in the conduction band is improve due to the electron-gaining and right shift of the Fermi level is happened, which in accordance well with the left shift of DOS. In conclusion, the electrical conductivity of Au–doped MoS_2 monolayer is greatly improved after adsorbing C_2H_4 molecule. Combined with the observation of **Figures 6B,C**, it can be found that the contributions of C_2H_4 to the DOS of system are at the energies of −17, −12, −9, −4, and 0.5 eV. The obvious overlapping peak Au-5d, C-2p, and H-1s orbitals at −6 eV displayed in **Figure 6D** reveals the strong hybridization among them, which elucidate the strong attraction of Au–doped MoS_2 monolayer to C_2H_4 molecule.

The large adsorption energy, larger transferred electrons, shorter adsorption distance and stronger orbitals hybridization perhaps reveal that the stronger interaction in Au-doped adsorption system than in MoS_2 monolayer adsorption structure. In consequence, the Au–doped MoS_2 monolayer is sensitive enough to detect C_2H_4 gas and it is able to be a potential sensing material for C_2H_4 sensors.

CONCLUSION

In this paper, the adsorption mechanism of C_2H_6 and C_2H_4 gases on MoS_2 based sensing materials were analyzed by the First-principles with DFT calculations. Firstly, the model of intrinsic MoS_2 monolayer was optimized and its structural parameters and electronic characteristics were calculated. It is found that MoS_2 monolayer with band gap of 2.058 eV is observed to be a direct band semiconductor. Then the adsorption of C_2H_6 and C_2H_4 molecules on MoS_2 monolayer were investigated, the corresponding structural parameters, charge transfer, adsorption energies and density of states were calculated

to obtain the adsorption capacity. The results show that the intrinsic MoS_2 monolayer cannot adsorb gas effectively. The Au atom was chose as the dopant to enhance the properties of MoS_2 monolayer and the bandgap of Au-doped MoS_2 monolayer is decreased to 0.266 eV, which indicates a promotion in the metallicity. In final, the adsorption structures of Au-doped MoS_2 monolayer to C_2H_6 and C_2H_4 molecules were modeled and the electronic structure of adsorption systems was investigated in detail. The adsorption energies to C_2H_6 and C_2H_4 are −0.463 and −0.952 eV, and the transferred charges from molecules to Au-doped MoS_2 monolayer are 0.118e and 0.309e, respectively. The impressive evidences from PDOS verify the hybridization between the orbitals of molecules and Au-doped MoS_2 monolayer, which implies the strong interaction between them. In addition, the increased conductivity after gases adsorption were indicated by the decreased band gap. Therefore, it is concluded that the Au doping promotes the adsorption capacity of MoS_2 monolayer to C_2H_6 and C_2H_4 molecules by influencing the electronic properties. In summary, the present study demonstrates the surface reactivity to C_2H_6 and C_2H_4 gases of MoS_2 based sensing materials, which is meaningful to develop the MoS_2 based gas sensors for the detection of C_2H_6 and C_2H_4 gases.

DATA AVAILABILITY STATEMENT

The raw data supporting the conclusions of this article will be made available by the authors, without undue reservation, to any qualified researcher.

AUTHOR CONTRIBUTIONS

All authors listed have made a substantial, direct and intellectual contribution to the work, and approved it for publication.

REFERENCES

Benounis, M., Aka-Ngnui, T., Jaffrezic, N., and Dutasta, J. P. (2008). NIR and optical fiber sensor for gases detection produced by transformation oil degradation. *Sens. Actuators A Phys.* 141, 76–83. doi: 10.1016/j.sna.2007.07.036

Chao, J. F., Chen, Y. H., Xing, S. M., Zhang, D. L., and Shen, W. L. (2019). Facile fabrication of ZnO/C nanoporous fibers and ZnO hollow spheres for high performance gas sensor. *Sens. Actuators B Chem.* 298:126927. doi: 10.1016/j.snb.2019.126927

Chatterjee, A., Bhattacharjee, P., Roy, N. K., and Kumbhakar, P. (2013). Usage of nanotechnology based gas sensor for health assessment and maintenance of transformers by DGA method. *Int. J. Electr. Power* 45, 137–141. doi: 10.1016/j.ijepes.2012.08.044

Chen, D. C., Tang, J., Zhang, X. X., Li, Y., and Liu, H. J. (2019a). Detecting decompositions of sulfur hexafluoride using MoS_2 monolayer as gas sensor. *IEEE Sens. J.* 19, 39–46. doi: 10.1109/JSEN.2018.2876637

Chen, D. C., Zhang, X. X., Tang, J., Cui, Z. L., and Cui, H. (2019b). Pristine and Cu decorated hexagonal InN monolayer, a promising candidate to detect and scavenge SF_6 decompositions based on first-principle study. *J. Hazard. Mater.* 363, 346–357. doi: 10.1016/j.jhazmat.2018.10.006

Chen, W. G., Zhou, Q., Gao, T. Y., Su, X. P., and Wan, F. (2013). Pd-doped SnO_2-based sensor detecting characteristic fault hydrocarbon gases in transformer oil. *J. Nanomater.* 2013, 2521–2535. doi: 10.1155/2013/127345

Chen, X., Wong, C. K. Y., Yuan, C. A., and Zhang, G. (2013). Nanowire-based gas sensors. *Sens. Actuators B Chem.* 177, 178–195. doi: 10.1016/j.snb.2012.10.134

Chen, Y. P., Wang, X. F., Shi, C. M., Li, L., Qin, H. W., and Hu, J. F. (2015). Sensing mechanism of SnO_2 (1 1 0) surface to H_2: density functional theory calculations. *Sens. Actuators B Chem.* 220, 279–287. doi: 10.1016/j.snb.2015.05.061

Cun, H., Chen, D. C., Zhang, Y., and Zhang, X. X. (2019). Dissolved gas analysis in transformer oil using Pd catalyst decorated $MoSe_2$ monolayer: a first-principles theory. *Sustain. Mater. Technol.* 17:e00094. doi: 10.1016/j.susmat.2019.e00094

de Lima, R. A., Soares, V. H., Martins, J. F., and Fontana, E. (2019). Tailoring a spectral line detection system for applications in dissolved gas analysis. *Sens. Actuators A Phys.* 293, 178–188. doi: 10.1016/j.sna.2019.04.020

Esrafili, M. D., and Rad, F. A. (2019). Carbon-doped boron nitride nanosheets as highly sensitive materials for detection of toxic NO and NO_2 gases: a DFT study. *Vacuum* 166, 127–134. doi: 10.1016/j.vacuum.2019.04.065

Kim, J. H., Mirzaei, A., Kim, H. W., and Kim, S. S. (2019). Realization of Au-decorated WS_2 nanosheets as low power-consumption and selective gas sensors. *Sens. Actuators B Chem.* 296:126659. doi: 10.1016/j.snb.2019.126659

Kim, J. H., Mirzaei, A., Kim, H. W., and Kim, S. S. (2020). Variation of shell thickness in ZnO-SnO_2 core-shell nanowires for optimizing sensing behaviors to CO, C_6H_6, and C_7H_8 gases. *Sens. Actuators B Chem.* 302:127150. doi: 10.1016/j.snb.2019.127150

Ma, G. M., Jiang, J., Li, C. R., Song, H. Y., Luo, Y. T., and Wang, H. B. (2015). Pd/Ag coated fiber Bragg grating sensor for hydrogen monitoring in power transformers. *Rev. Sci. Instrum.* 86:045003. doi: 10.1063/1.4918802

Ma, H., Saha, T. K., Ekanayake, C., and Martine, D. (2015). Smart transformer for smart grid-intelligent framework and techniques for power transformer asset management. *IEEE. Trans. Smart. Grid.* 2, 1026–1034. doi: 10.1109/TSG.2014.2384501

Nobrega, L. A. M. M., Xavier, G. V. R., Aquino, M. V. D., Serres, A. J. R. C. C. R., Albuquerque, C. C. R., and Costa, E. G. (2019). Design and development of a bio-inspired UHF sensor for partial discharge detection in power transformers. *Sensors* 19:653. doi: 10.3390/s19030653

Qian, H., Lu, W. H., Wei, X. X., Chen, W., and Deng, J. (2019). H_2S and SO_2 adsorption on Pt-MoS_2 adsorbent for partial discharge elimination: a DFT study. *Results Phys.* 12, 107–112. doi: 10.1016/j.rinp.2018.11.035

Qin, Y., and Ye, Z. (2016). DFT study on interaction of NO_2 with the vacancy-defected WO_3 nanowires for gas-sensing. *Sens. Actuators B Chem.* 222, 499–507. doi: 10.1016/j.snb.2015.08.040

Suryavanshi, H., Velandy, J., and Sakthivel, M. (2017). Wavelet power ratio signature spectrum analysis for prediction of winding insulation defects in transformer and shunt reactor. *IEEE Trans. Dielectr. Electr. Insul.* 24, 2649–2659. doi: 10.1109/TDEI.2017.006328

Uddin, A. S. M. I., Yaqoob, U., and Chung, G. S. (2016). Dissolved hydrogen gas analysis in transformer oil using Pd catalyst decorated on ZnO nanorod array. *Sens. Actuators B Chem.* 226, 90–95. doi: 10.1016/j.snb.2015.11.110

Wang, J., Jiang, S. S., Liu, H. L., Wang, S. H., Pan, Q. J., Yin, Y. D., et al. (2020). P-type gas-sensing behavior of Ga_2O_3/Al_2O_3 nanocomposite with high sensitivity to NO_x at room temperature. *J. Alloy. Compd.* 814:152284. doi: 10.1016/j.jallcom.2019.152284

Wang, J. X., Zhou, Q., Lu, Z. R., Gui, Y. G., and Zeng, W. (2019b). Adsorption of H_2O molecule on TM (Au, Ag) doped-MoS_2 monolayer: a first-principles study. *Physica E* 113, 72–78. doi: 10.1016/j.physe.2019.05.006

Wang, J. X., Zhou, Q., Lu, Z. R., Wei, Z. J., and Zeng, W. (2019c). Gas sensing performances and mechanism at atomic level of Au-MoS_2 microspheres. *Appl. Surf. Sci.* 490, 124–136. doi: 10.1016/j.apsusc.2019.06.075

Wang, J. X., Zhou, Q., and Zeng, W. (2019a). Competitive adsorption of SF_6 decompositions on Ni-doped ZnO (100) surface: computational and experimental study. *Appl. Surf. Sci.* 479, 185–197. doi: 10.1016/j.apsusc.2019.01.255

Wang, X. H., Wang, D. W., Yang, A. J., Koratkar, N., Chu, J. F., Lv, P. L., et al. (2018). Effects of adatom and gas molecule adsorption on the physical properties oftellurene: a first principles investigation. *Phys. Chem. Chem. Phys.* 20, 4058–4066. doi: 10.1039/C7CP07906K

Wen, M. Q., Xiong, T., Zang, Z. G., Wei, W., Tang, X. T., and Dong, F. (2016). Synthesis of MoS_2/g-C_3N_4 nanocomposites with enhanced visible-light photocatalytic activity for the removal of nitric oxide (NO). *Opt. Express* 24, 10205–10212. doi: 10.1364/OE.24.010205

Yang, F., Jung, D., and Penner, R. M. (2011). Trace detection of dissolved hydrogen gas in oil using a palladium nanowire array. *Anal. Chem.* 83, 9472–9477. doi: 10.1021/ac2021745

Zahra, K. (2018). Evaluation of H_2S sensing characteristics of metals–doped graphene and metals-decorated graphene: insights from DFT study. *Physica E* 99, 261–268. doi: 10.1016/j.physe.2018.02.022

Zhang, D. Z., Jiang, C. X., Li, P., and Sun, Y. E. (2017a). Layer-by-layer self-assembly of Co_3O_4 nanorod-decorated MoS_2 nanosheet-based nanocomposite toward high-performance ammonia detection. *ACS. Appl. Mater. Inter.* 9, 6462–6471. doi: 10.1021/acsami.6b15669

Zhang, D. Z., Jiang, C. X., and Wu, J. F. (2018). Layer-by-layer assembled In_2O_3 nanocubes/flower-like MoS_2 nanofilm for room temperature formaldehyde sensing. *Sens. Actuators B Chem.* 273, 176–184. doi: 10.1016/j.snb.2018.06.044

Zhang, D. Z., Sun, Y. E., Jiang, C. X., and Zhang, Y. (2017b). Room temperature hydrogen gas sensor based on palladium decorated tin oxide/molybdenum disulfide ternary hybrid via hydrothermal route. *Sens. Actuators B Chem.* 242, 15–24. doi: 10.1016/j.snb.2016.11.005

Zhang, D. Z., Wu, J. F., Li, P., and Cao, Y. H. (2017c). Room-temperature SO_2 gas sensing properties based on metal-doped MoS_2 nanoflower: an experimental and density functional theory Investigation. *J. Mater. Chem. A*, 5, 20666–20677. doi: 10.1039/C7TA07001B

Zhang, Y. J., Zeng, W., and Li, Y. Q. (2018). Hydrothermal synthesis and controlled growth of hierarchical 3D flower-like MoS_2 nanospheres assisted with CTAB and their NO_2 gas sensing properties. *Appl. Surf. Sci.* 455, 276–282. doi: 10.1016/j.apsusc.2018.05.224

Zhao, C. J., and Wu, H. R. (2018). A first-principles study on the interaction of biogas with noble metal (Rh, Pt, Pd) decorated nitrogen doped graphene as a gas sensor: a DFT study. *Appl. Surf. Sci.* 435, 1199–1212. doi: 10.1016/j.apsusc.2017.11.146

Zhou, Q., Chen, W. G., Xu, L. N., Kumarc, R., Gui, Y. G., Zhao, Z. Y., et al. (2018a). Highly sensitive carbon monoxide (CO) gas sensors based on Ni and Zn doped SnO_2 nanomaterials. *Ceram. Int.* 44, 4392–4399. doi: 10.1016/j.ceramint.2017.12.038

Zhou, Q., Hong, C. X., Yao, Y., Hussain, S., Xu, L. N., Zhang, Q. Y., et al. (2018b). Mingsong Wang, Hierarchically MoS_2 nanospheres assembled from nanosheets for superior CO gas-sensing properties. *Mater. Res. Bull.* 101, 132–139. doi: 10.1016/j.materresbull.2018.01.030

Zhou, Q., Umar, A., Sodki, E. M., Amine, A., Xu, L. N., Gui, Y. G., et al. (2018c). Fabrication and characterization of highly sensitive and selective sensors based on porous NiO nanodisks. *Sens. Actuators B Chem.* 259, 604–615. doi: 10.1016/j.snb.2017.12.050

Zhou, Q., Xu, L. N., Umar, A., Chen, W. G., and Kumar, R. (2018d). Pt nanoparticles decorated SnO_2 nanoneedles for efficient CO gas sensing applications. *Sens. Actuators B Chem.* 256, 656–664. doi: 10.1016/j.snb.2017.09.206

Zhou, Q., Zeng, W., Chen, W. G., Xu, L. N., Kumar, R., and Umar, A. (2019). High sensitive and low-concentration sulfur dioxide (SO_2) gas sensor application of heterostructure NiO-ZnO nanodisks. *Sens. Actuators B Chem.* 298:126870. doi: 10.1016/j.snb.2019.126870

Conflict of Interest: The authors declare that the research was conducted in the absence of any commercial or financial relationships that could be construed as a potential conflict of interest.